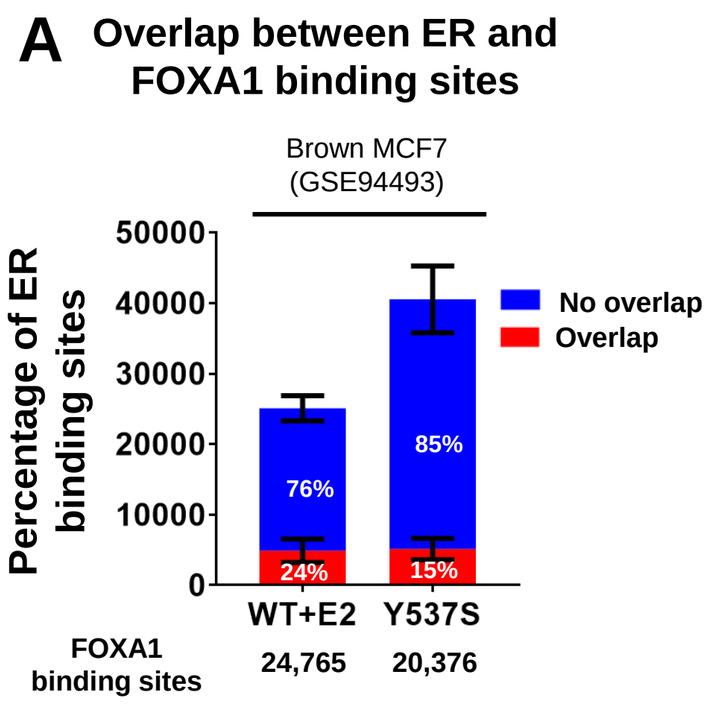

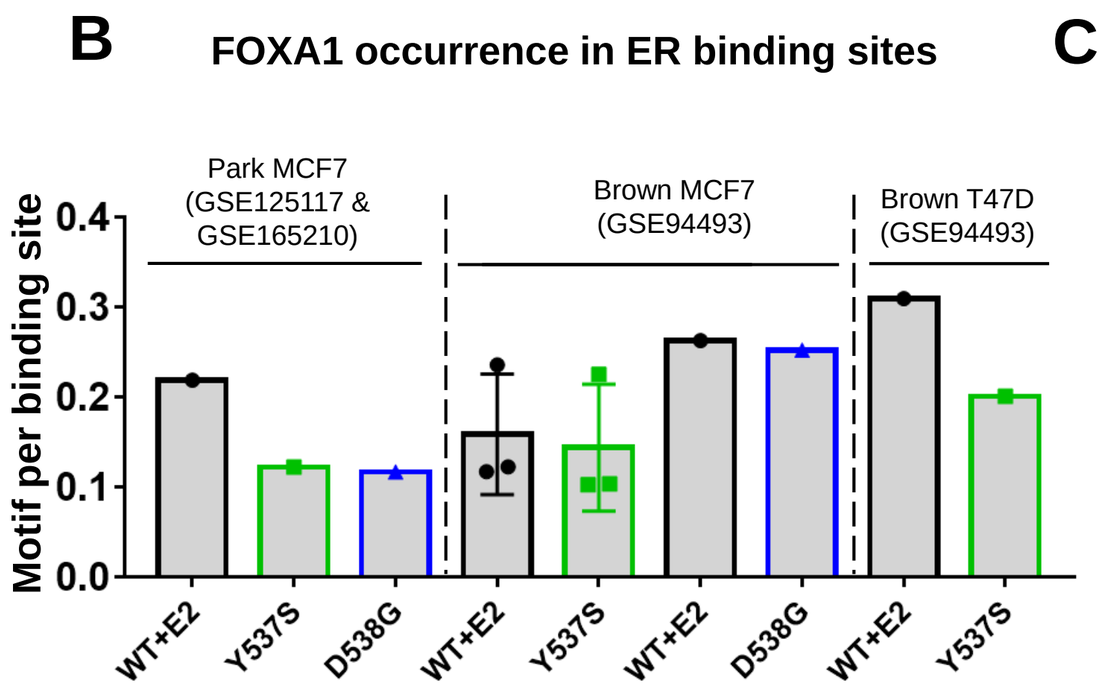

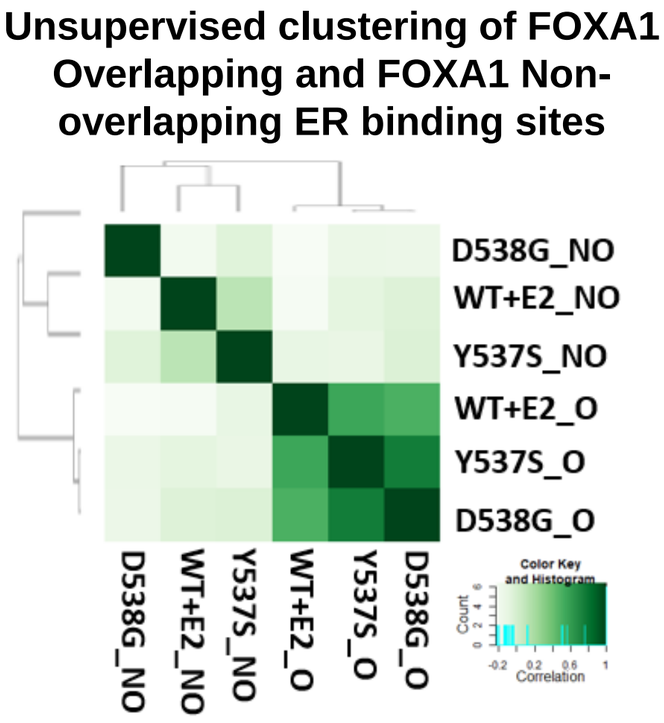

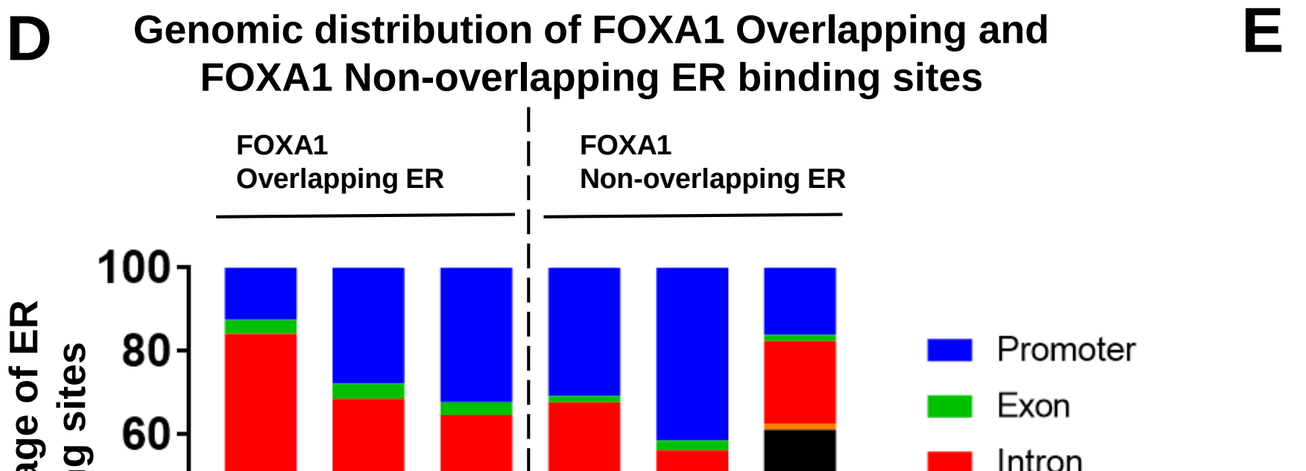

E

FOXA1 Overlapping ER binding sites

	Y537S vs. WT+E2	D538G vs. WT+E2
Promoter	↑ (p<0.0001)	↑ (p<0.0001)
Exon	— (p=0.7393)	— (p=1)
Intron	↓ (p=0.0023)	↓ (p=0.0003)
3'/5' UTR	— (p=1)	— (p=0.6518)
Distal intergenic	↓ (p=0.0231)	↓ (p=0.006)

FOXA1 Non-overlapping ER binding sites

	Y537S vs. WT+E2	D538G vs. WT+E2
Promoter	↑ (p<0.0001)	↓ (p<0.0001)
Exon	— (p=0.3244)	— (p=1)
Intron	↓ (p=0.0185)	↓ (p<0.0001)
3'/5' UTR	— (p=1)	— (p=0.6518)
Distal intergenic	↓ (p=0.0241)	↑ (p<0.0001)

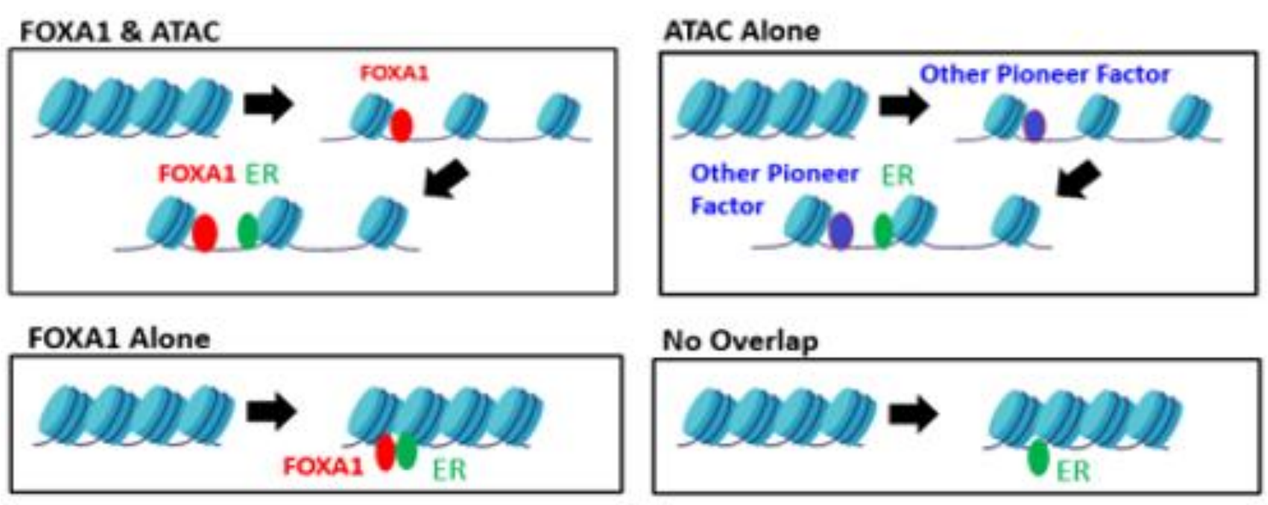

Supplementary Figure S1. FOXA1 redistribution in *ESR1* mutant cells causes distinct ER-FOXA1 interaction.

(A) Bar plot representing the percentage of ER binding sites overlapping with FOXA1 binding sites in Brown MCF7 cells. Each bar represents mean ± SD with three biological replicates.

(B) Bar plot representing the percentage of FOXA1 motifs present in the ER binding sites in Park MCF7, Brown MCF7 and T47D cells. Each bar represents mean ± SD with three biological replicates.

(C) Heatmap showing the unsupervised clustering of FOXA1 Overlapping ER and FOXA1 Non-overlapping ER binding sites. The 'O' and 'NO' in the figure mean overlapping sites and non-overlapping sites respectively.

(D) Stacked bar plot showing the genomic distribution of FOXA1 Overlapping ER and FOXA1 Non-overlapping ER binding sites.

(E) The statistic difference of each genomic region between *ESR1* mutant and WT cells, the p-values were obtained by Fisher's exact test.

(F) Schematic plot showing the four FOXA1-ER-chromatin interaction patterns corresponding to four conditions analyzed in Figure. 1E.

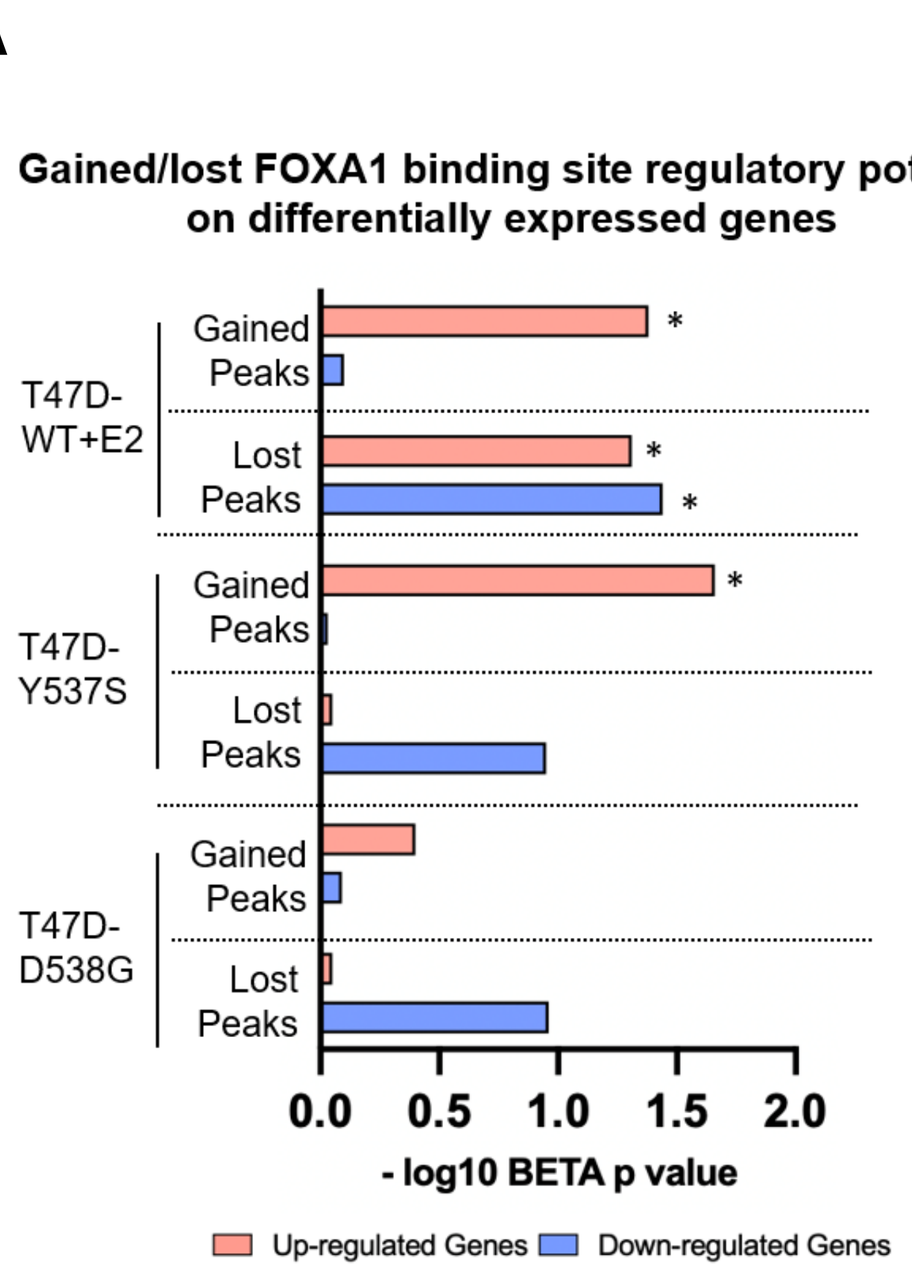

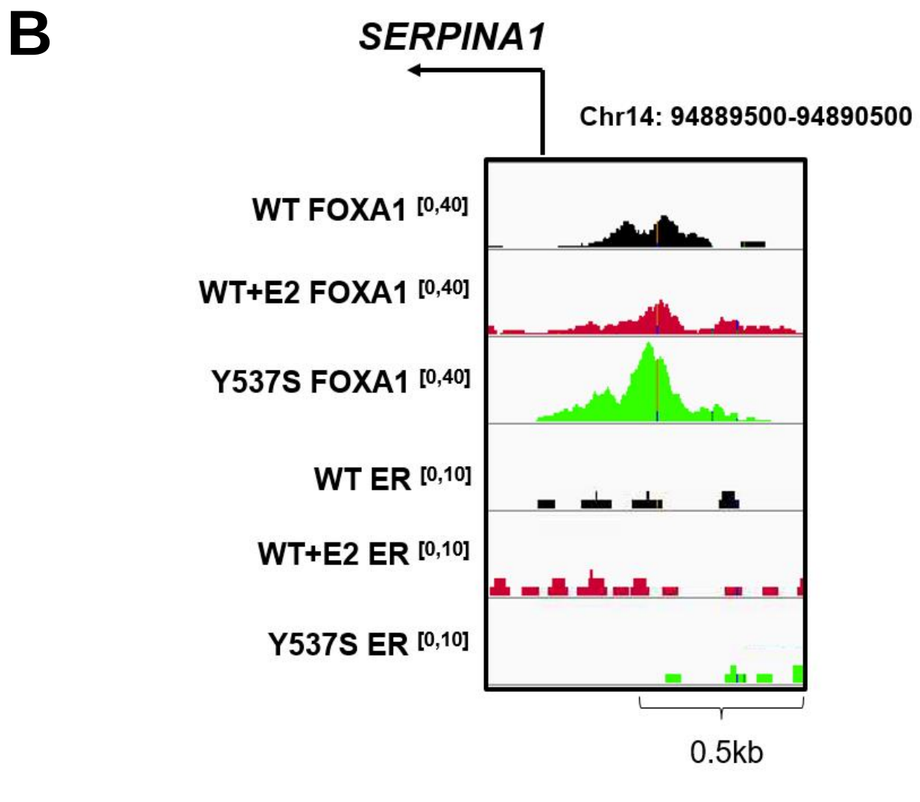

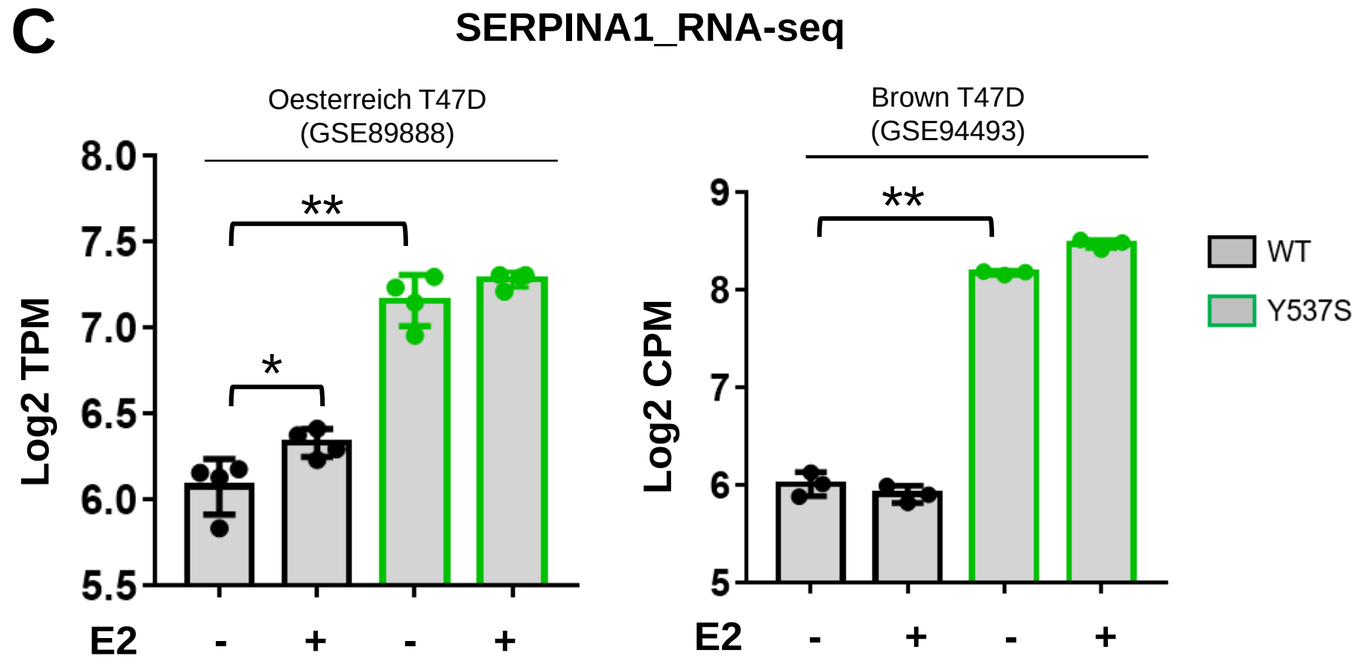

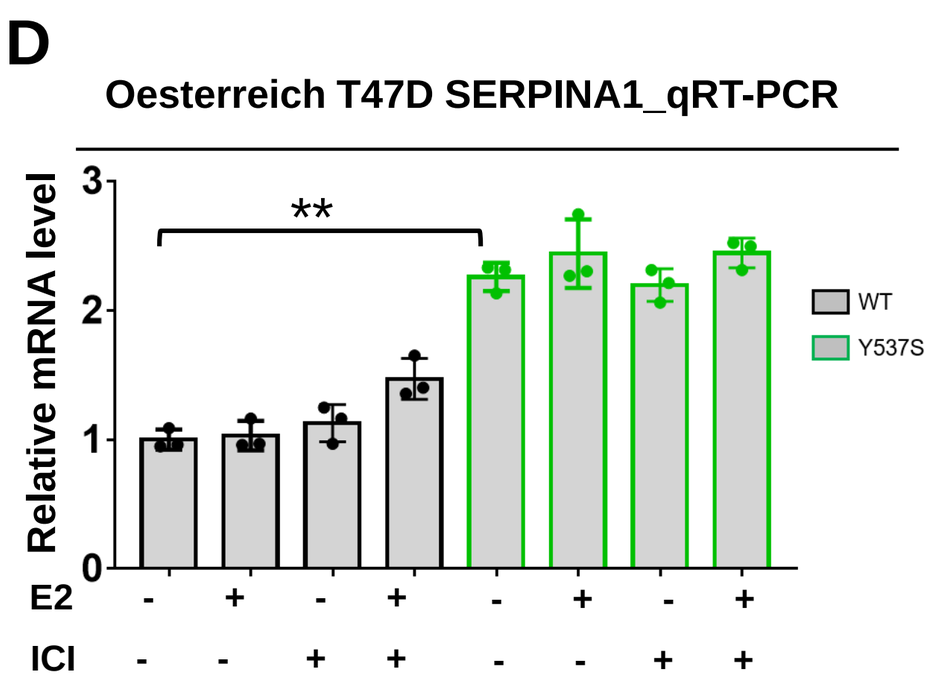

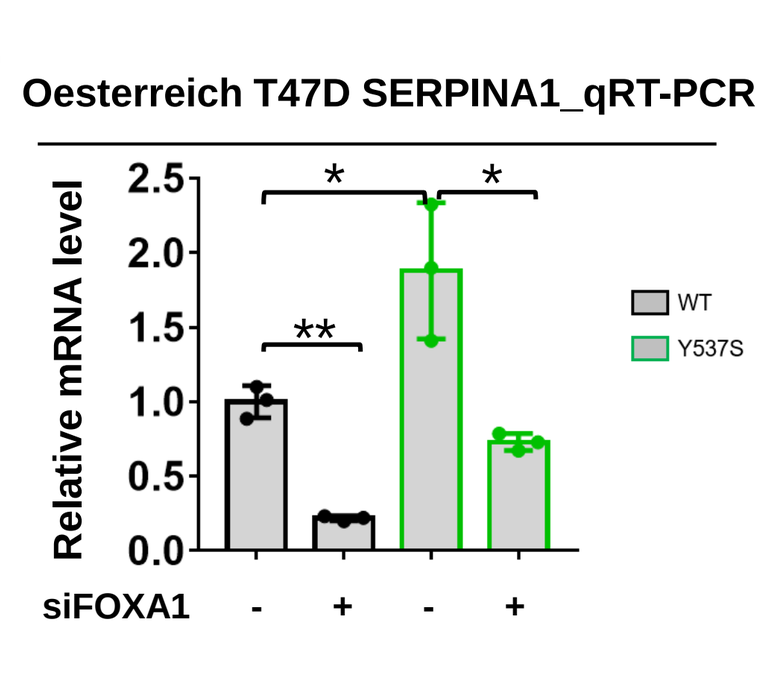

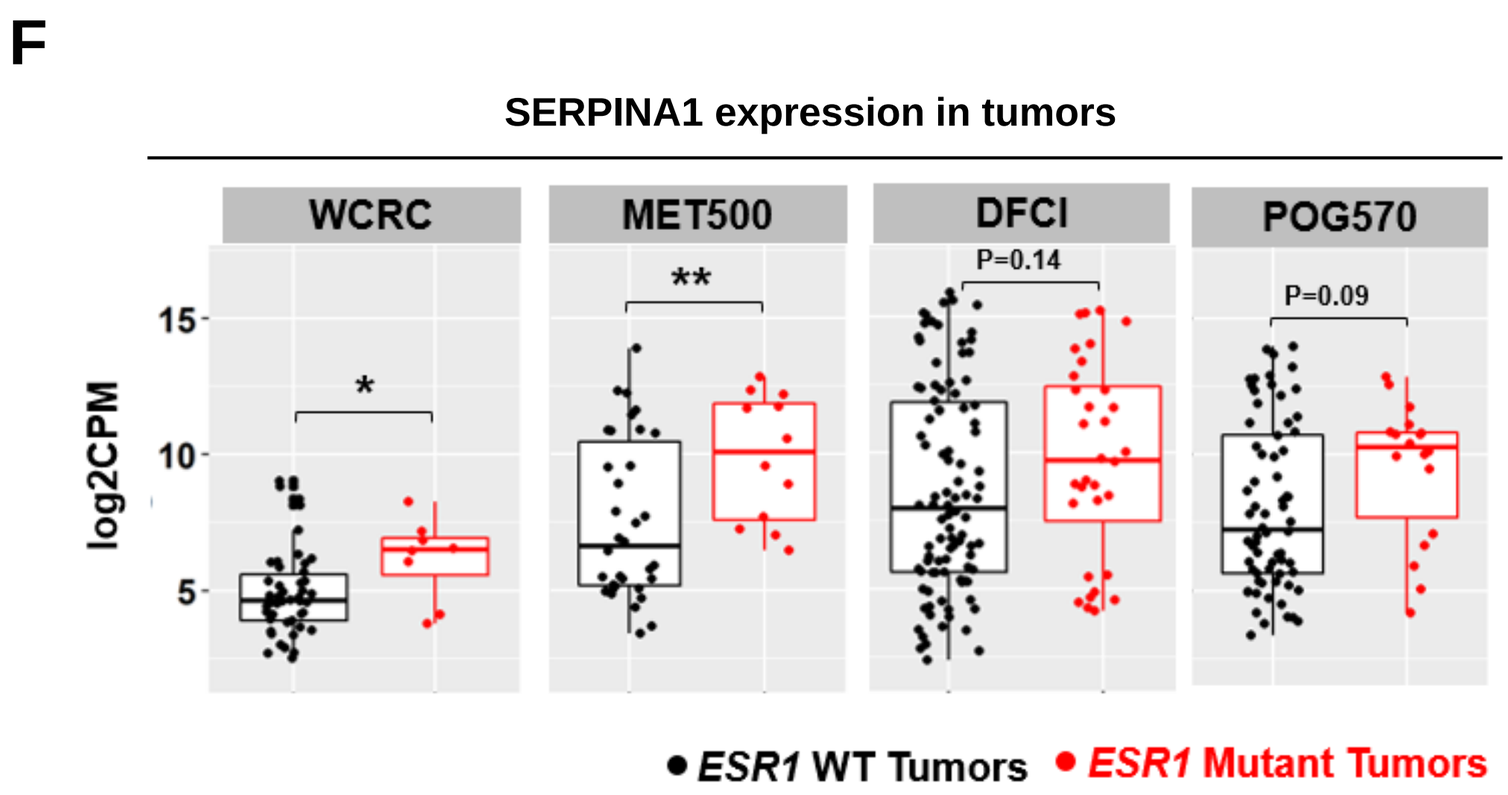

Supplementary Figure S2. FOXA1 gained peaks annotated genes are significantly associated with novel target genes.

Supplementary Figure S2-Continued

Supplementary Figure S2. FOXA1 gained peaks annotated genes are significantly associated with novel target genes.
(A) Bar plot showing the regulatory potential of gained/lost FOXA1 peaks on differentially expressed genes in T47D WT+E2, Y537S and D538G cells. p values were obtained by one-tailed Kolmogorov-Smirnov test from BETA. (* $p<0.05$)
(B) Genomic track showing FOXA1 and ER binding intensities at *SERPINA1* locus of T47D WT, WT+E2 and Y537S cells. Y-axis show the name of each group with reads intensity scale on the upper left.
(C) Bar plot showing the expression of *SERPINA1* in Oesterreich and Brown T47D cells based on RNA-seq data. Each error bar represents mean ± SD with three biological replicates. Student's t test was used to compare the expression between Y537S and WT cells, and between E2 and Veh treatment. (* $p<0.05$, ** $p<0.01$)
(D) qRT-PCR measurement of *SERPINA1* mRNA level in Oesterreich T47D WT and Y537S cells with Veh or 1nM E2 or 1μM ICI or 1nM E2 + 1μM ICI treatment. mRNA fold changes were normalized to RPLP0 and further normalized to WT Veh group. Each bar represents mean ± SD with three biological replicates. Student's t test was used to compare the expression between Y537S and WT cells. Dunnett's test was used to compare the expression between control and treatment groups. (** $p<0.01$)
(E) qRT-PCR measurement of *SERPINA1* mRNA level in Oesterreich T47D WT and mutant cells after FOXA1 siRNA knockdown. mRNA fold changes were normalized to RPLP0 and further normalized to WT cells. Each bar represents mean ± SD with three biological replicates. Student's t test was used to compare the expression between Y537S and WT cells, and between scramble and knockdown groups. (** $p<0.01$)
(F) Box plots representing the expression of SERPINA1 in *ESR1* mutant versus *ESR1* WT metastatic tumors in four ER+ metastatic breast cancer cohorts. (WCRC, 46 WT/8 mutant; MET500, 34 WT/12 mutant; DFCI, 98 WT/32 mutant; POG570, 68 WT/18 mutant). Box plots span the upper quartile (upper limit), median (centre) and lower quartile (lower limit). Whiskers extend a maximum of 1.5X IQR. Mann-Whitney U test was used to compare the log2CPM of SERPINA1 in WT and mutant tumors. (* $p<0.05$, ** $p<0.01$)

Supplementary Figure S3

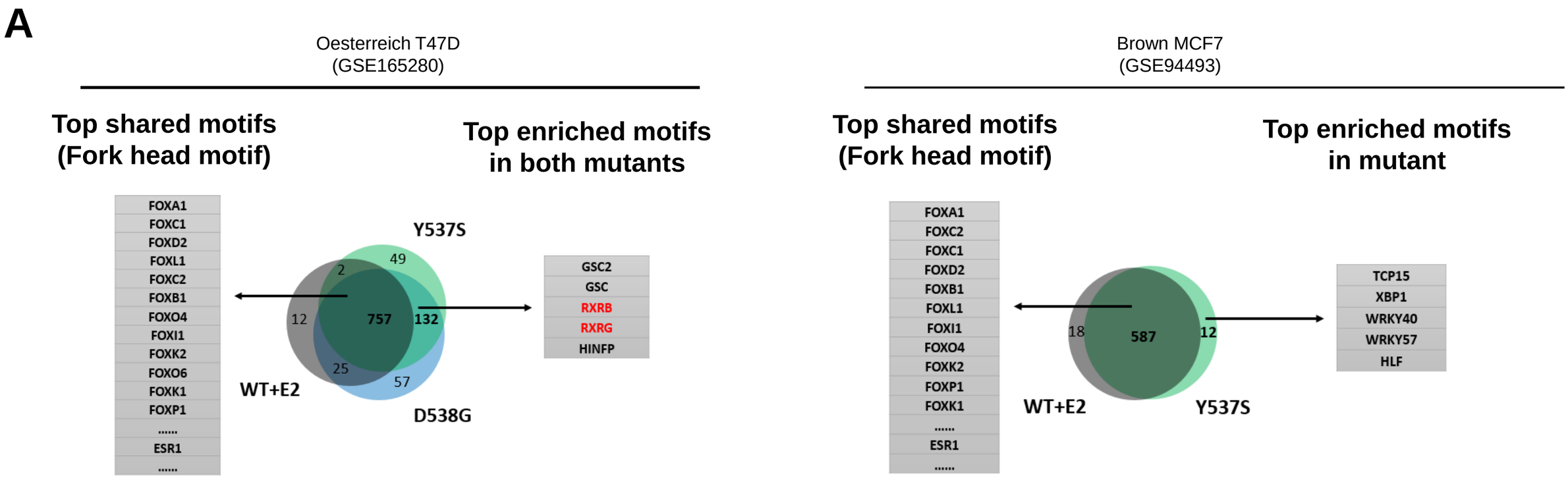

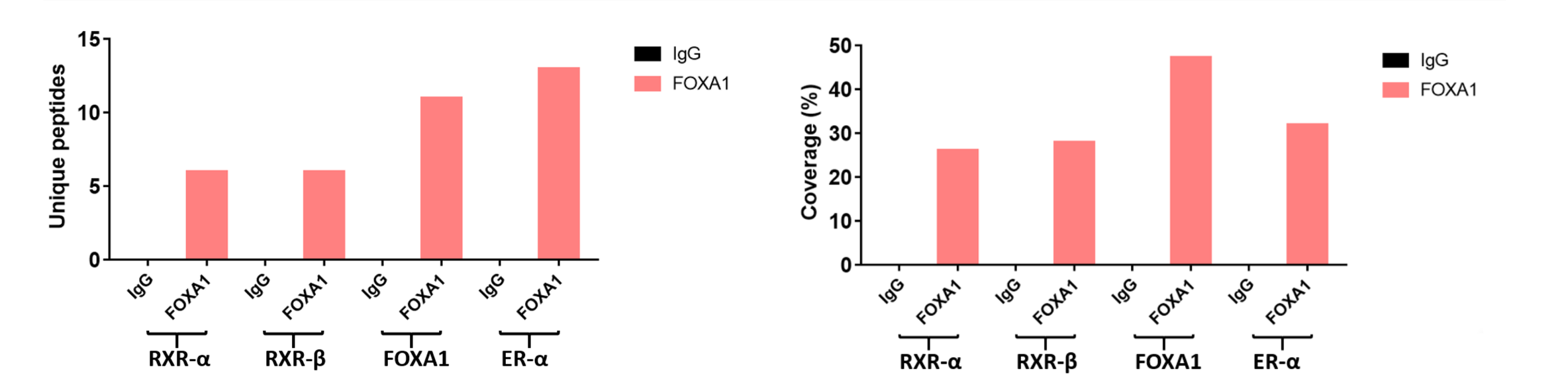

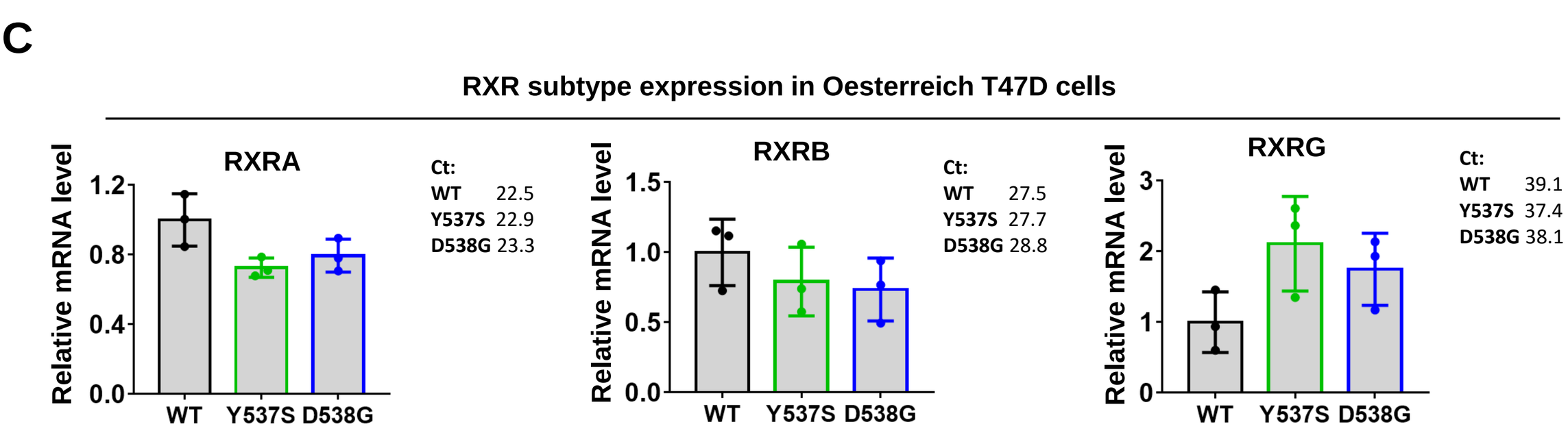

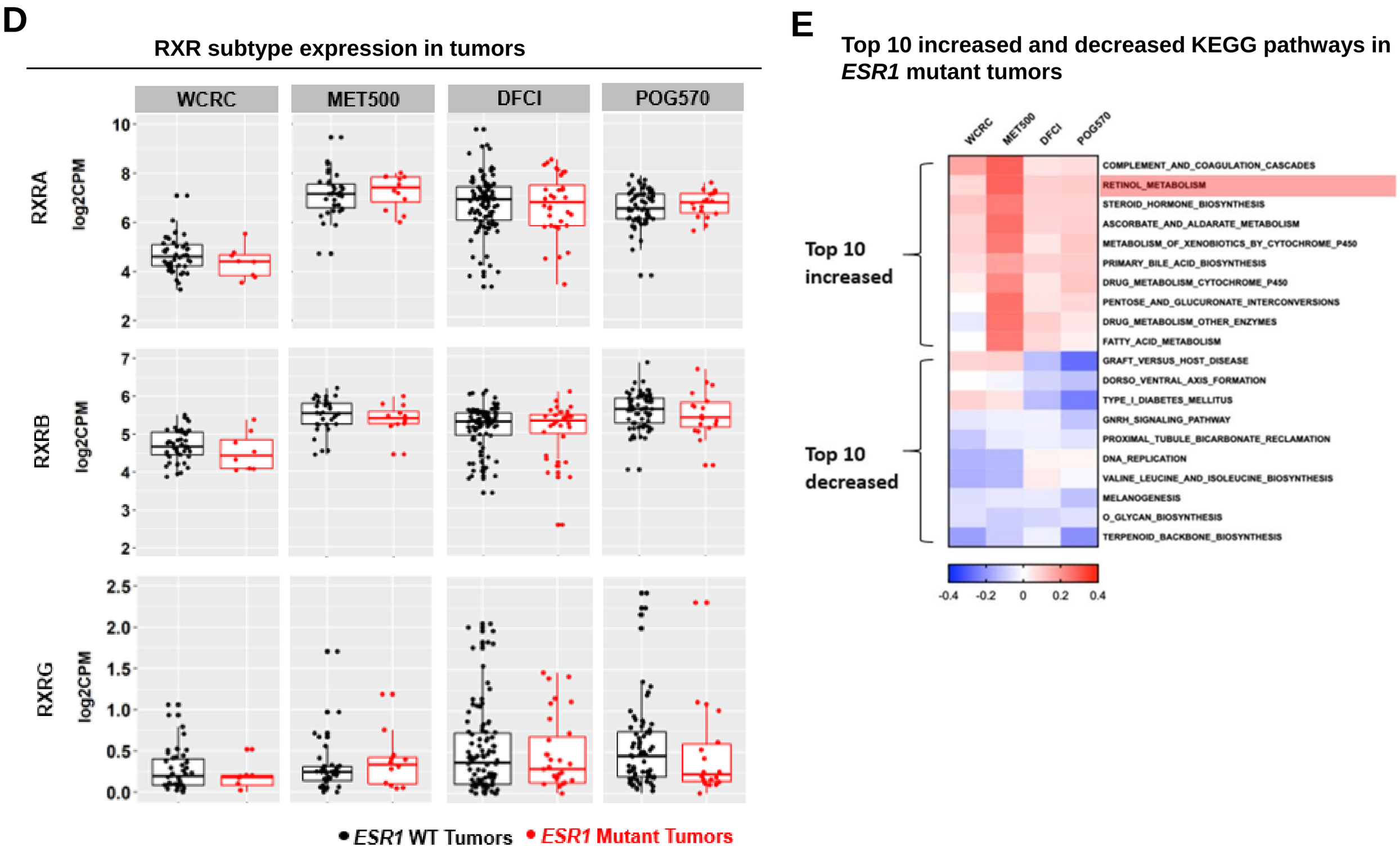

Supplementary Figure S3. FOXA1 redistribution in *ESR1* mutant cells confers potential RXR binding sites.

Supplementary Figure S3-Continued

Supplementary Figure S3. FOXA1 redistribution in *ESR1* mutant cells confers potential RXR binding sites.
(A) Motif enrichment analysis of FOXA1 binding sites in Brown MCF7 and Oesterreich T47D cells. Venn diagram shows the overlap of significantly enriched motifs (MEME-Suite E-value<0.05) in Oesterreich T47D WT+E2, Y537S and D538G cells (left panel), and Brown MCF7 WT+E2 and Y537S cells (right panel). The top shared motifs and mutant-enriched motifs were shown on each side, motifs of RXR subtypes were highlighted.
(B) MCF7 FOXA1 rapid immunoprecipitation mass spectrometry of endogenous proteins (RIME) data showing the unique peptides (left panel) and coverage (right panel) of RXR-α, RXR-β, FOXA1 and ER-α. IgG control IP group and FOXA1 IP group were shown.
(C) qRT-PCR measurement of *RXRA*, *RXRB* and *RXRG* mRNA level in Oesterreich T47D WT and mutant cells. mRNA fold changes were normalized to RPLP0 and further normalized to WT cells. Each bar represents mean ± SD with three biological replicates. Ct values were highlighted on the right side.
(D) Box plots representing the expression of RXRA, RXRB and RXRG in *ESR1* WT and mutant metastatic tumors in four ER+ metastatic breast cancer cohorts (WCRC, 46 WT/8 mutant; MET500, 34 WT/12 mutant; DFCI, 98 WT/32 mutant; POG570, 68 WT/18 mutant). Box plots span the upper quartile (upper limit), median (centre) and lower quartile (lower limit). Whiskers extend a maximum of 1.5X IQR.
(E) Heatmap representing the top 10 increased and decreased KEGG pathways in *ESR1* mutant tumors identified by gene set variation analysis (GSVA) in four ER+ metastatic breast cancer cohorts (WCRC, 46 WT/8 mutant; MET500, 34 WT/12 mutant; DFCI, 98 WT/32 mutant; POG570, 68 WT/18 mutant).

Supplementary Figure S4

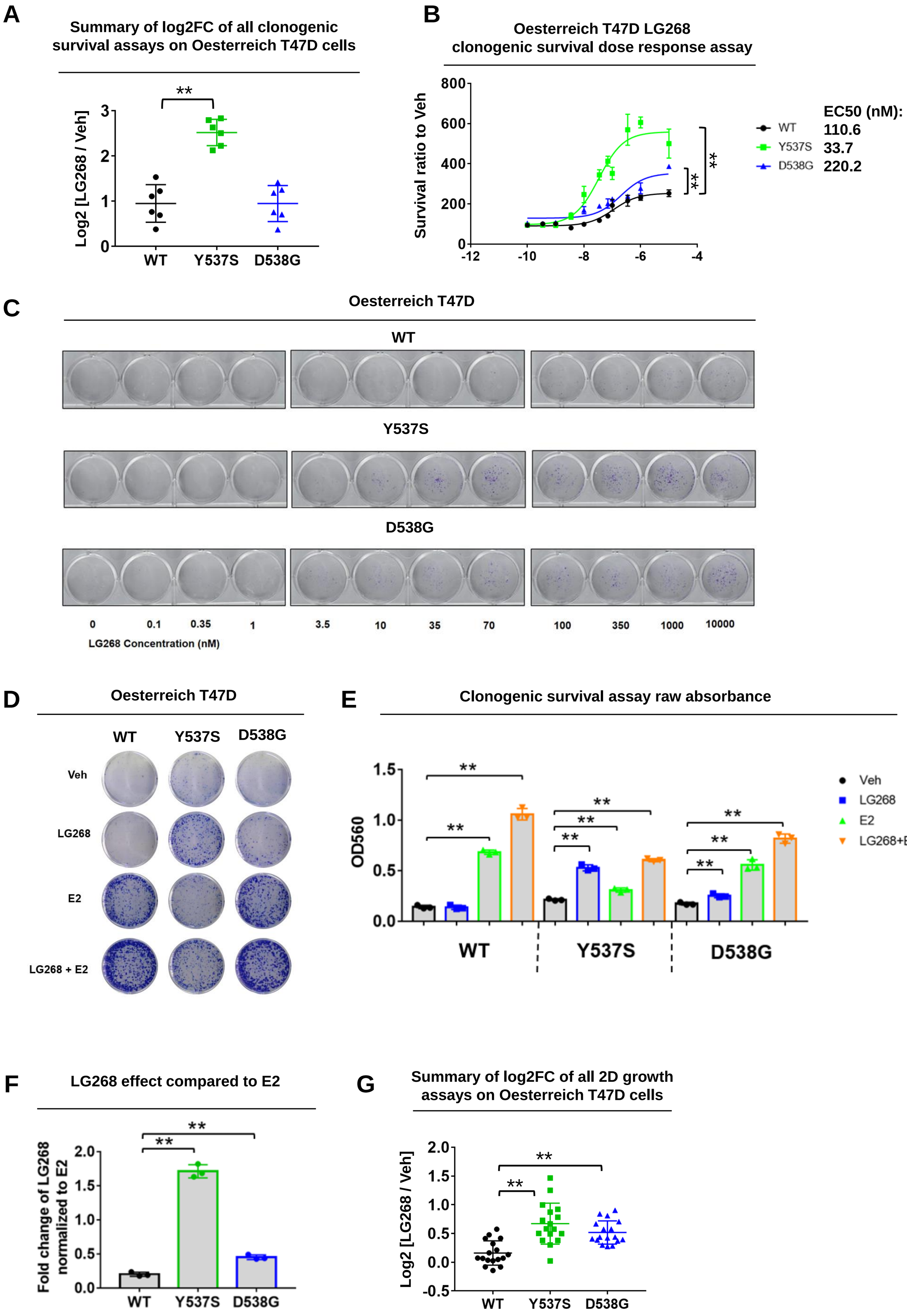

Supplementary Figure S4. RXR agonist LG100268 can promote colonization and growth of *ESR1* mutant cells

Supplementary Figure S4-Continued

Supplementary Figure S4. RXR agonist LG100268 can promote colonization and growth of *ESR1* mutant cells

(A) Summary of all colony formation assay results on Oesterreich T47D cells, log2 fold changes by normalizing OD560 of LG268 group to Veh group were extracted from 6 independent experiments displayed as mean ± SD. Dunnett's test was used to compare between WT and mutant cells. (* $p<0.05$, ** $p<0.01$) (Related to Figure 2B)

(B, C) LG268 colony formation dose response assay on Oesterreich T47D cells. (B) The raw absorbance OD560 was obtained after crystal violet staining and acetic acid dissolving, normalized to Veh and presented as fold change. Each bar represents mean ± SD with three biological replicates.EC50s were shown on the right side. Two-way ANOVA test was performed to compare the dose response between mutant and WT cells. (** $p<0.01$) (C) Representative images of colonies formed after different doses of LG268 treatment.

(D) Representative images of colonies formed after Veh or 100nM LG268 or 1nM E2 or 100nM LG268 + 1nM E2 treatment in hormone deprived condition with Oesterreich T47D models for 14 days.

(E) Bar plot showing the quantification of (D) with raw absorbance OD560 of each group after crystal violet staining. Each bar represents mean ± SD with three biological replicates. Student's t test was used to examine the effects of treatment between each group's OD560 (** $p<0.01$).

(F) Bar plot showing the fold change of OD560 in LG268 group normalized to that in E2 group for three cells. Each bar represents mean ± SD with three biological replicates. Student's t test was used to examine the difference between mutants and WT (** $p<0.01$).

(G) Summary of all growth assay results on Oesterreich T47D cells, log2 fold changes at day 7 were extracted from 17 independent experiments displayed as mean ± SD. Dunnett's test was used to compare between WT and mutant cells. (* $p<0.05$, ** $p<0.01$) (Related to Figure 2E)

Supplementary Figure S5

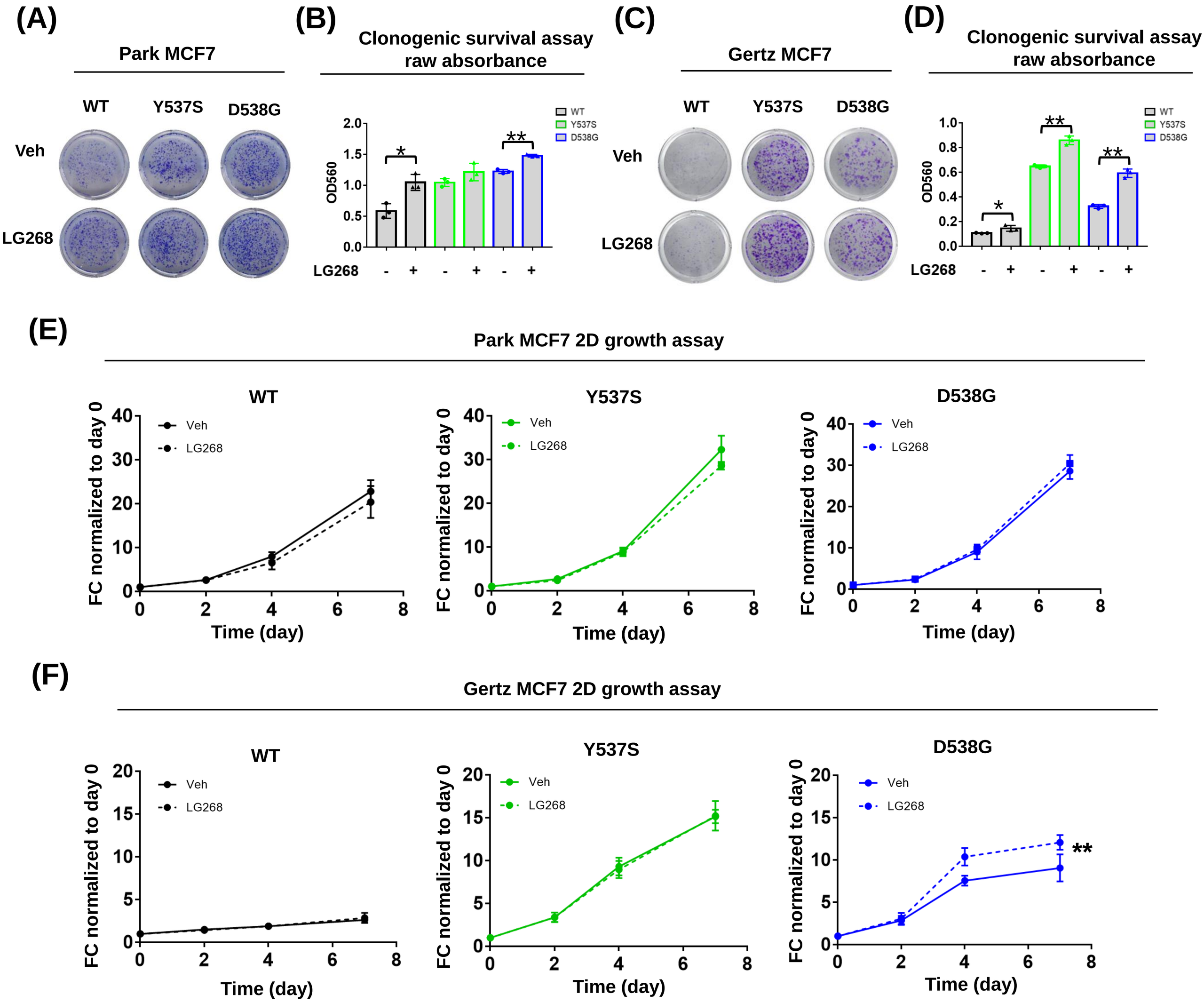

Supplementary Figure S5. Clonogenic survival assay and 2D growth assay to test RXR response in Park and Gertz MCF7 cell models.

(A, C) Representative images of colonies formed after Veh or 100nM LG268 treatment in hormone deprived condition with Park (A) and Gertz (C) models for 14 days.

(B, D) Bar plot showing the quantification of A and C with raw absorbance OD560 of each group after crystal violet staining. Each bar represents mean ± SD with three biological replicates. Student's t test was used to examine the effects of treatment between each group's OD560. (** p<0.01)

(E, F) Growth curve of Park (E) and Gertz (F) MCF7 cells under Veh or 100nM LG268 treatment in hormone deprived condition. Cell amount quantified by FluoReporter kit at day 7 was normalized to day 0 and presented as fold change (FC). Each bar represents mean ± SD with five biological replicates. Two-way ANOVA was performed to compare the 100nM LG268 group and Veh group. (** p<0.01)

Supplementary Figure S6

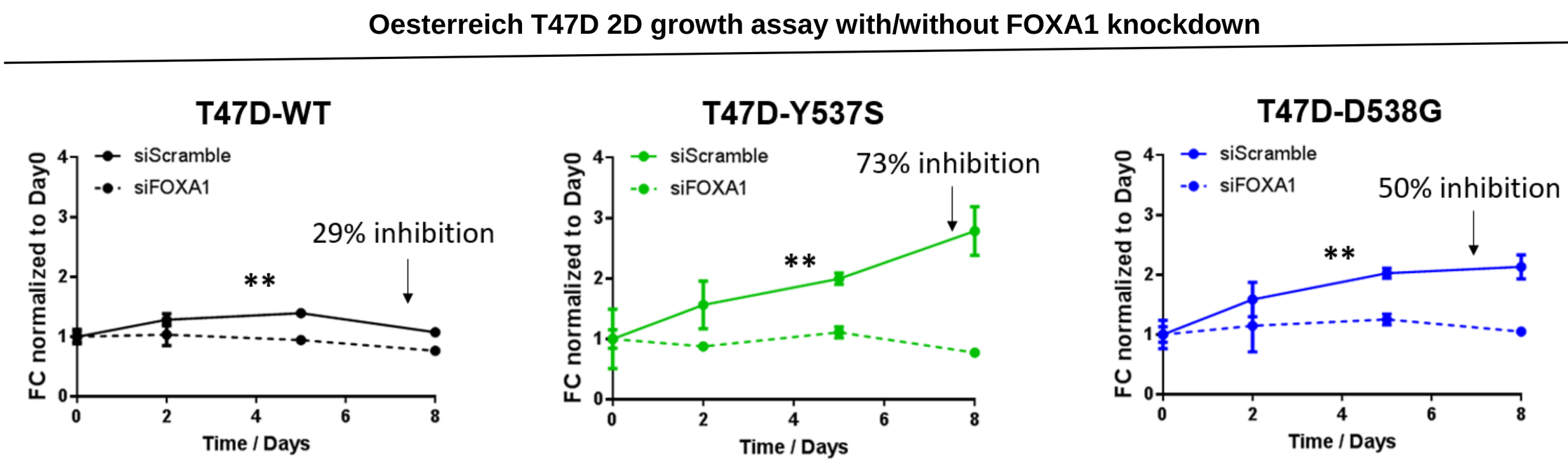

Supplementary Figure S6. FOXA1 knockdown drastically attenuated the base line growth of both *ESR1* WT and mutant cells.

Growth curve of T47D cells after Scramble or FOXA1 siRNA treatment in hormone deprived condition. Cell amount quantified by FluoReporter kit at day 7 was normalized to day 0 and presented as fold change (FC). Each bar represents mean ± SD with five biological replicates. Two-way ANOVA was performed to compare the siFOXA1 group and siScramble group. (** $p<0.01$).

Supplementary Figure S7

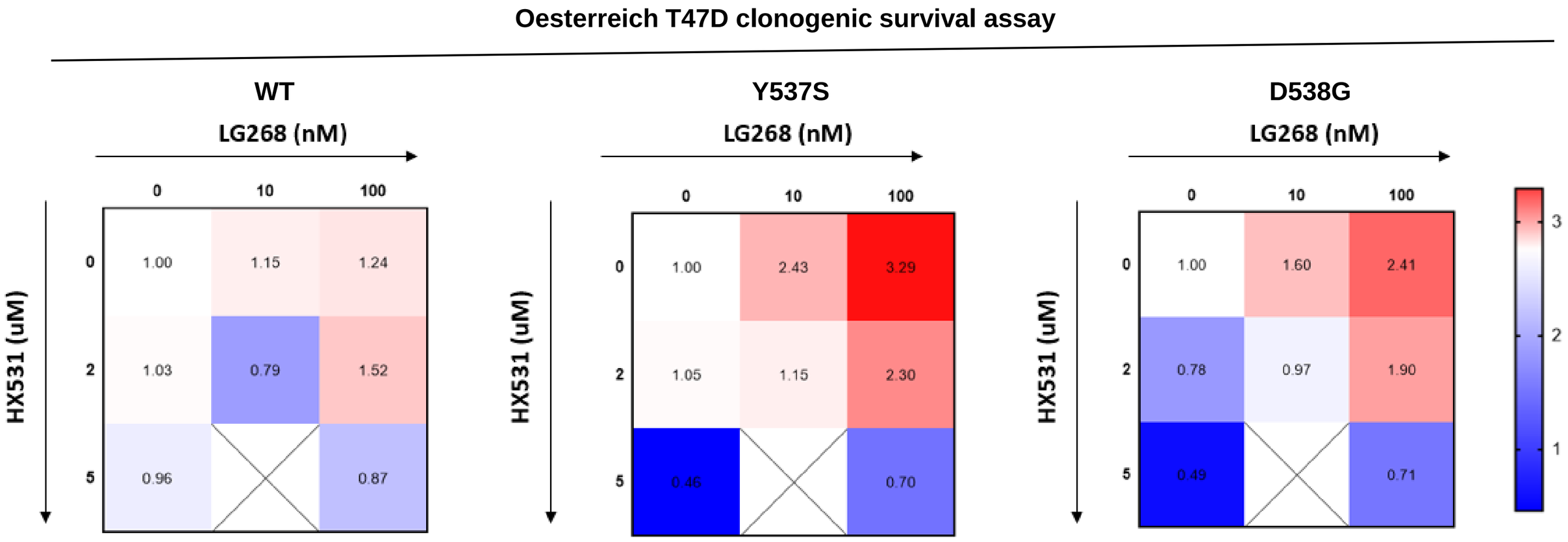

Supplementary Figure S7. RXR antagonist HX531 can inhibit the response of *ESR1* mutant cells to RXR agonist.

Clonogenic survival assay result of Oesterreich T47D cells treated with the corresponding combined doses of LG268 and HX531. The raw absorbance OD560 was obtained after crystal violet staining and acetic acid dissolving, and normalized to Veh group as fold change (FC). Heatmaps represent the FCs after different treatment in WT, Y537S and D538G cells. Due to plate restriction, the condition with 10nM LG268 + 5 μM HX531 was not performed and labeled ‘X’ in the figure.

Supplementary Figure S8

A

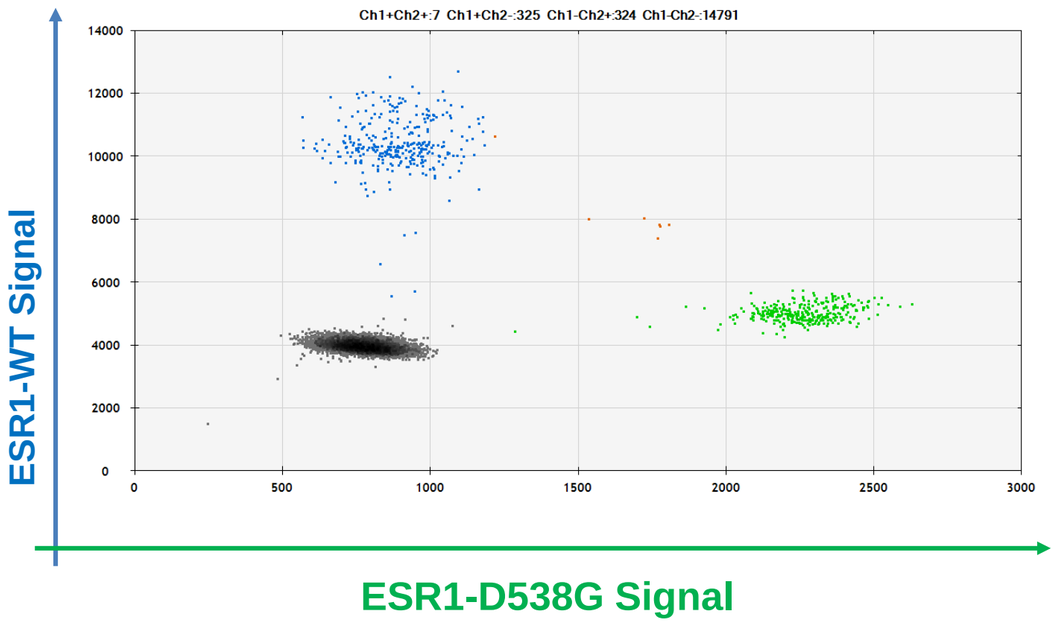

B

Gene	Average Ct value
RPLP0	20.00
RXRA	25.69
RXRB	38.47
RXRG	NA

Supplementary Figure S8. RXR antagonist HX531 can inhibit the basal and agonist promoted growth of IPM-PDXO-073 organoid.
(A) 2D scatter plots showing ddPCR validation of DNA mutation allele frequency in IPM-PDXO-073 organoid. Black dots reflect no DNA droplet, blue and green dots show droplets containing solely WT or D538G DNA, orange dots represent droplets containing both WT and mutant DNA copies. (B) qRT-PCR check of basal level of RXRA, RXRB and RXRG in IPM-PDXO-073 organoid. Average Ct values were indicated in the table, RPLP0 was used as internal control. Each bar represents mean ± SD with three biological replicates.